

## Reactor Vessel Heating by the Natural Convection of the Melted Core in Three-Layer Configuration

Ji-Won Bae and Bum-Jin Chung\*

Department of Nuclear Engineering, Kyung Hee University

#1732 Deogyong-daero, Giheung-gu, Yongin-si, Gyeonggi-do, 17104, Republic of Korea

\*Corresponding author:bjchung@khu.ac.kr

### 1. Introduction

In a hypothetical severe accident of nuclear power plant, IVR-ERVC (In-Vessel Retention of molten corium via External Reactor Vessel Cooling) is a very desirable strategy to guarantee the integrity of the vessel by flooding the reactor cavity. To adopt this strategy, reactor vessel heating by the natural convection of the core melts should be sufficiently cooled by ERVC. Therefore, it is necessary to know the heat load imposed on the vessel [1, 2].

The molten corium could be stratified into two- or three-layer configuration by density difference. In case of three-layer configuration, the thickness of light metal layer is thinner than two-layer one due to the additional heavy metal layer. The thinner light metal layer intensifies the heat focusing to the reactor vessel. Therefore, it is more important to investigate natural convection of the oxide layer in three-layer configuration. However, only a few studies have been carried out on three-layer configuration. Furthermore, experiments were conducted only on two-dimensional (2-D) facilities, although the flow patterns in oxide layer vary depending on the dimensions of facility [3]. To understand the heat load caused by natural convection in oxide layer that is most similar to one in practice, experiments with three-dimensional (3-D) facility need to be conducted.

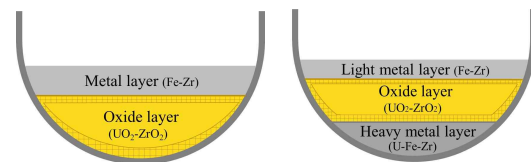
This study conducted the natural convection experiments on the oxide layer in three-layer configuration, using 3-D facilities of various heights. Mass transfer experiments were performed using copper sulfuric acid ( $\text{CuSO}_4\text{-H}_2\text{SO}_4$ ) electroplating system based on the analogy concept between heat and mass transfer. We measured local heat transfer coefficients ( $h_h$ ) at the top and bottom plates simulating the interface between light and heavy metal layers and oxide layer, respectively. Also, 3-D experimental results were compared with 2-D results of preceding studies [4, 5]. The  $Ra'_H$  varied from  $2.06 \times 10^{12}$  to  $6.90 \times 10^{13}$ . The  $Sc$ , which corresponds to  $Pr$  was 2,014.

### 2. Theoretical background

#### 2.1. Basic phenomena for oxide layer

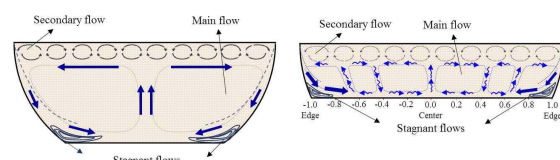
When the nuclear fuel melts due to failure of sufficient cooling, it relocates to the reactor vessel

and stratifies into two- or three-layer configuration according to the accident scenarios. For two-layer configuration as shown in Fig. 1(a), the metal layer consists of metallic materials (Fe, Zr), and the oxide layer contains oxidized materials ( $\text{UO}_2$ ,  $\text{ZrO}_2$ ). If there is enough un-oxidized Zr in the metal layer, the U in oxide layer migrates to the metal layer to form a heavy alloy. Then, large density of this alloy induces layer inversion and three-layer configuration is formed (Fig 1(b)). The heavy metal layer consists of U, Fe, and Zr with some metallic fission products.



(a) Two-layer configuration (b) Three-layer configuration  
Fig. 1. The composition of layer according to the configuration type [5].

Especially in three-layer configuration, Bae and Chung [5] presented the flow patterns in the 2-D oxide layer (Fig. 2). In Fig. 2(a), the natural convection flows run down along the curved cooling wall by ERVC. Then, flows merge at center of the bottom plate and rise to the top plate, and finally split up toward the edge. It is a symmetrical 'twin-cell' flow. When the depth of oxide layers becomes shallow, the number of cell increases, which forms 'multi-cell' flow (Fig. 2(b)). For the 3-D oxide layer, these flow patterns also change into 3-D, resulting in the different heat transfer phenomena in the oxide layer [3]. Moreover, this difference in flow pattern between 2- and 3-D facilities would be expected to intensify, particularly in the shallow layer forming the multi-cell flow. In addition, the cooling from the top plate induces the natural convective flows called secondary flows underneath the top plate.



(a) Twin-cell (b) Multi-cell  
Fig. 2. Flow pattern for three-layer configuration according to the aspect ratio [5].

## 2.2. Definition of $Ra'_H$

As the oxide layer generates decay heat continuously due to the radioactive fission products, the natural convection of the oxide layer is special as it imposes the heat load on the reactor vessel. Therefore, to consider the volumetric heat generation ( $q'''$ ), the modified Rayleigh number ( $Ra'_H$ ) is expressed as the multiplication of the conventional Rayleigh number ( $Ra_H$ ) and Damköhler number ( $Da_H$ ). The  $Da_H$  is a dimensionless number considering the presence of volumetric (internal) heat generation ( $q'''$ ). The  $Ra'_H$  is expressed by

$$Ra'_H = Ra_H \times Da_H = \frac{g\beta\Delta TH^3}{\alpha\nu} \times \frac{q'''H^2}{k\Delta T} = \frac{g\beta q''' H^5}{\alpha\nu k}, \quad (1)$$

$$\text{where } Da_H = \frac{q'''H^2}{k\Delta T}. \quad (2)$$

## 2.3. Previous studies

Segal *et al.* [6] performed the heat transfer experiments using 2-D semi-circular facility. The paraffin oil (upper layer), water (middle layer) and chlorobenzene (lower layer) were used for simulating three-layer configuration and their heights are 0.05 m, 0.18 m, 0.04 m respectively. They located the heater to entire middle layer and part of upper layer to simulate the internal heat source. The  $Ra'_H$  varies from  $6.01 \times 10^{12}$  to  $7.82 \times 10^{12}$ . The heat load on the reactor vessel increased with the angle until the middle of the oxide layer. It does not explain for the heat focusing from the upper metal layer to the vessel.

Kim *et al.* [3] investigated the natural convection of 2-D oxide pool in two-layer configuration and compared with that of 3-D oxide pool. They conducted mass transfer experiments using the MassTER-OP2 (Mass Transfer Experimental Rig for a 2-D Oxide Pool). The radius and height are 0.1 m and the width is 0.04 m. The  $Ra'_H$  varied from  $1.49 \times 10^{12}$  to  $1.36 \times 10^{13}$ . They reported that the 2-D experimental results were not affected by  $Ra'_H$  whereas 3-D one varied with  $Ra'_H$  due to the influence of the geometry.

Kim and Chung [4], and Bae and Chung [5] studied the influence of the aspect ratio ( $H/R$ ) on the reactor vessel heating through the mass transfer experiments. The height of MassTER-OP2(HML) is varied to 0.028 m, 0.038 m, 0.047 m, 0.056 m and 0.078 m, which corresponds the  $Ra'_H$  from  $6.70 \times 10^{10}$  to  $4.30 \times 10^{13}$ . They confirmed that the multi-cell flow formed in small  $H/R$  lower than 0.47 using the measured local average currents.

## 3. Experiments

### 3.1. Experimental methodology of mass transfer

Heat and mass transfer systems are analogous as

their governing equations are mathematically same. Therefore, by the mass transfer experiments, the heat transfer problems can be solved effectively [7].

The copper sulfate-sulfuric acid ( $\text{CuSO}_4\text{-H}_2\text{SO}_4$ ) electroplating system was adopted and in this system, to calculate the mass transfer coefficient ( $h_m$ ), we used the limiting current technique. It developed by several researchers [8-11], and the methodology is well-established [12-14]. In this study, the measured total current ( $I_{tot}$ ) at all electrodes simulates to the internal heat generation ( $q$ ) in oxide layer.

By the mass transfer experiments, we could achieve the various characteristics of oxide layer properly: high  $Ra'_H$  with small facilities, uniform heat generation and isothermal cooling condition without heat leakage.

### 3.2. Experimental apparatus

Fig. 3 shows the MassTER-OP3(HML) (Mass Transfer Experimental Rig for a 3-D Oxide Pool with Heavy Metal Layer). They have same radius and height with previous MassTER-OP2(HML) [4, 5]. The radius is 0.1 m and the heights are 0.047 m, 0.056 m and 0.078 m. The  $Ra'_H$  is varied from  $2.06 \times 10^{12}$  to  $6.93 \times 10^{13}$ . The inner wall of the top, curved side and bottom were made up with the cathode copper plates. The halves of cathode are single electrodes. The other halves were divided up into ten electrodes in radial ring shape to measure the local average current. The cruciform anode copper that simulates internal heat sources was located in the center of the facility, which was adopted by referring to the results of comparative test on the volumetric heat source [13]. The facilities were filled with copper sulfate-sulfuric acid ( $\text{CuSO}_4\text{-H}_2\text{SO}_4$ ) solution.

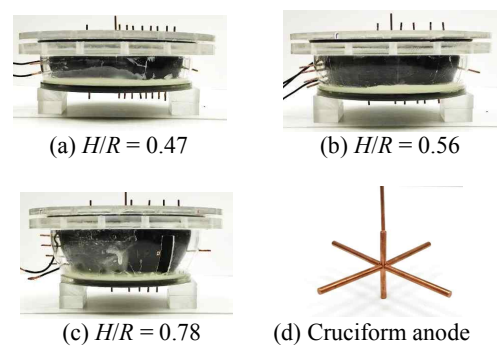


Fig. 3. Experimental apparatus.

While carrying out the IVR-ERVC strategy, downward flow is formed along the curved wall by external cooling. However, for the electroplating system, upward flow is caused as the cathode simulates a heated wall due to the reduction of cupric ions at the cathode causing the decrease of fluid density and resulting upward buoyancy. Therefore, the direction of gravity must be reversed to simulate

the downward flow with electroplating system. Thus, the experiments were performed with the inverted circuit as shown in Fig. 4 and some earlier studies conducted with this kind of circuit well agreed with existing correlations [13-14].

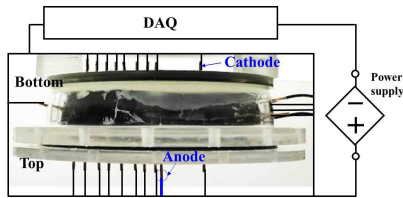


Fig. 4. Test circuit.

### 3.3. Test matrix

Table I is test matrix for this experiments. With the fixed isothermal condition of the sidewall, the top and bottom boundary condition were varied for four different cooling conditions, which simulates the extreme cooling situation. The real conditions in severe accident will be included between these extrema.

Table I: Test matrix.

Boundary condition			$Sc (Pr)$
Side	Top	Bottom	
Isothermal	Isothermal	Isothermal	2,014
		Insulated	
	Insulated	Isothermal	
		Insulated	

## 4. Results and Discussions

Fig. 5 presents the normalized local heat transfer coefficients at the bottom plate ( $h_{bottom}^*$ ) varying the aspect ratios ( $H/R$ ) for isothermal condition in all surfaces. For all  $H/R$ ,  $h_{bottom}^*$  decreases from the center to the edge. However, the decrease tendencies are quite different according to the  $H/R$ . In the large aspect ratio such as  $H/R = 0.78$ ,  $h_{bottom}^*$  gradually decreases toward the edge after the early steep decline, which means the formation of twin-cell flow. On the other hand, when the  $H/R$  decreases less than or equal to 0.56, tendency of  $h_{bottom}^*$  shows wavy distribution, which means the formation of multi-cell flow. They are not corresponding with 2-D experimental results of Bae and Chung [5] that the multi-cell flow began to form when the  $H/R$  is less than 0.47. Since the 2-D and 3-D flows are not same, it seems that the influence of  $H/R$  on the flow pattern in the oxide layer is also not same.

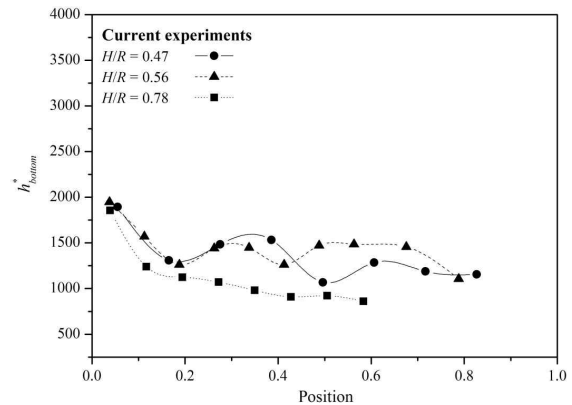


Fig. 5. Normalized downward local heat transfer coefficients ( $h_{bottom}^*$ ) according to  $H/R$ .

Fig. 6 exhibits the normalized local heat transfer coefficients at the top plate ( $h_{top}^*$ ) varying the bottom boundary condition and  $H/R$ . The top heat transfer also differs with 2-D experimental results. It is highest at the center as the 3-D flow is stronger than 2-D flow. The lot of downward flows along the sidewall merged at the center and would be pushed up in speed. Also,  $h_{top}^*$  rapidly decreases from the center to about position = 0.3 as 3-D flow disperses radially along the top plate and slow down. This cannot be investigated in the 2-D experimental results as the 2-D flow proceeds linearly along the top plate.

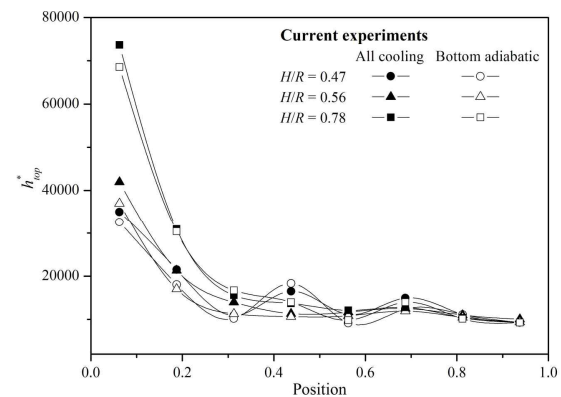


Fig. 6. Normalized upward heat transfer coefficients ( $h_{top}^*$ ) according to  $H/R$ .

Fig. 7 shows the ratios of upward heat to total heat ( $Q_{up}^*/Q_{tot}^*$ ), which are the measured results for 2-D and 3-D experiments with various  $H/R$ . For the 3-D experiments in this study, the  $Q_{up}^*/Q_{tot}^*$  is nearly constant regardless of  $H/R$  unlike 2-D experiment which shows combination of increase and constant trend. It seems that the dissimilarity between 2- and 3-D flows caused in different heat load on the top plate. In addition,  $Q_{up}^*/Q_{tot}^*$  for the shallow  $H/R$  of 3-D oxide layer is lower than 2-D one. Especially for the 3-D flows, it seems that effect of heat dispersion

by multi-cell appears to be greater than 2-D flows as 3-D flow is composed with many cells.

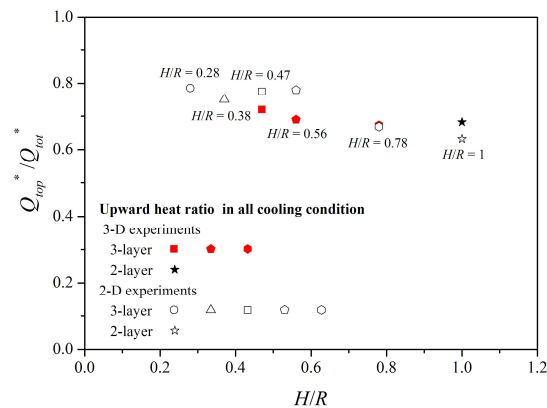


Fig. 7. Comparison of ratios of upward heat to total heat ( $Q_{up}^*/Q_{tot}^*$ ) between the 2- and 3-D experiments and  $H/R$ .

### 5. Conclusion

This study performed the 3-D experiments of natural convection of the oxide layer in three-layer configuration and confirmed the difference with the 2-D experiments. Based on analogy between heat and mass transfer, we conducted the mass transfer experiments using a copper sulfate-sulfuric acid ( $CuSO_4-H_2SO_4$ ) electroplating system.

For the downward local heat transfer, it was confirmed that, the flow regimes of the oxide layer were varied depending on the dimension of the facility. In addition, for 3-D experiments, the transition from twin-cell flow to multi-cell flow occurred at a larger  $H/R$  compared with 2-D ones. The upward local heat transfers of 3-D experiments decreased steeply with the distance from the center while those for 2-D ones decreased gently. It caused by differing flow regimes between 2-D and 3-D geometries. For the ratio of upward heat to the total heat, it investigated that the number of cell in 3-D flow seems to be more than that in 2-D flow, which results in enhancing the heat dispersing effect by the multi-cell.

The heat load from the 3-D oxide layer to the light and heavy metal layer was inconsistent with that from the 2-D oxide layer. It means that the 2-D experiment has limitation for simulating the heat transfer phenomena of a 3-D oxide layer.

### ACKNOWLEDGEMENT

This study was sponsored by the Ministry of Science and ICT (MSIT) and was supported by Nuclear Research & Development program grant funded by the National Research Foundation (NRF) (Grant code: 2017M2A8A4015283).

### REFERENCES

- [1] Theofanous, T.G. *et al.*, In-Vessel Coolability and Retention of a Core melt. Nuclear Engineering and Design 169 (1997) 1-48.
- [2] Park, S.D. *et al.*, Heat Removal Characteristics of IVR-ERVC Cooling System using Gallium Liquid Metal. NURETH 16, Chicago IL, 2015.
- [3] Kim, S.H. *et al.*, Two- and Three-Dimensional Experiments for Oxide Pool in In-Vessel Retention of Core Melts, Nuclear Engineering and Technology 49 (2017) 1405-1413.
- [4] Kim, S.H., Chung, B.J., Mass Transfer Experiments on the Natural Convection Heat Transfer of the Oxide Pool in a Three-Layer Configuration, Progress in Nuclear Energy 106 (2018) 11-19.
- [5] Bae, J.W., Chung, B.J., Development of Multi-Cell Flows in the Three-Layered Configuration of Oxide Layer and Their Influence on the Reactor Vessel Heating, Nuclear Engineering and Technology (in progress).
- [6] B. R. Sehgal *et al.*, Natural convection heat transfer in a stratified melt pool with volumetric heat generation, 6th International topical meeting on nuclear reactor thermal hydraulics, operations and safety (NUTHOS-6), Nara, Japan, 2004.
- [7] A. Bejan, Convection heat transfer. third ed, New York: John Wiley & Sons, INC, pp. 96-97, 173-179, 197-200, 512-516, 2006.
- [8] V.G. Levich, Physicochemical Hydrodynamics, Prentice-Hall, Englewood Cliffs, New Jersey, 1962.
- [9] J.N. Agar, Diffusion and convection at electrodes, Discuss. Faraday Soc. Vol. 26, pp. 27-37, 1947.
- [10] C.W. Tobias, R.G. Hickman, Ionic mass transfer by combined free and forced convection, Int. J. Res. Phys. Chem. Chem. Phys Vol. 229, pp. 145-166, 1965.
- [11] E.J. Fenech, C.W. Tobias, Mass transfer by free convection at horizontal electrodes, Electrochim. Acta 2, pp. 311-325, 1960.
- [12] Bae *et al.*, Visualization of natural convection heat transfer inside an inclined circular pipe, International Communications in Heat and Mass Transfer, Vol. 92, pp. 15-22, 2018.
- [13] Park *et al.*, Variation in the angular heat flux of the oxide pool with Rayleigh number, Annals of Nuclear Energy, Vol. 170, pp. 128-135, 2017.
- [14] Kim and Chung, Heat load imposed on reactor vessel during in-vessel retention of core melts, Nuclear Engineering and Design, Vol. 308, pp. 1-8, 2016